Available online at www.sciencedirect.com
SCIENCE DIRECT®
Journal of Crystal Growth 274 (2005) 126–131
JOURNAL OF CRYSTAL GROWTH
www.elsevier.com/locate/jcrysgro

Well-aligned zinc oxide nanorods and nanowires prepared without catalyst

F. Liu[a], P.J. Cao[a,b], H.R. Zhang[a], C.M. Shen[a], Z. Wang[a,c], J.Q. Li[a], H.J. Gao[a,*]

[a]*Institute of Physics, Chinese Academy of Science, Beijing 100083, PR China*
[b]*Department of Material Science & Engineering, School of Science, Shenzhen University, Guangdong 518060, PR China*
[c]*Northeastern University, Shenyang 110004, PR China*

Received 22 June 2004; accepted 22 September 2004
Communicated by R.S. Feigelson
Available online 30 October 2004

Abstract

Without catalyst and at a low temperature (550 °C), well-aligned ZnO nanorods and nanowires were prepared on porous silicon substrates using a simple method. Scanning electron microscopy (SEM) and transmission electron microscopy (TEM) results confirm that both the nanorods and the nanowires are perfect single crystals with the wurtzite structure. The diameters range from 40 to 100 nm. The growth directions are along the [0 0 0 1] axis. Photoluminescence (PL) spectra show that the UV emission shifts slightly to low frequency and the intensity of green emission decreases with the improvement of ZnO crystallization.

PACS: 81.07.−b; 81.16.Dn; 81.16.−c

Keywords: A1. Characterization; A3. Thermal evaporation method; B1. Nanowire; B1. Nanorod; B1. ZnO; B2. Oxide semiconducting materials

1. Introduction

In recent years, there has emerged significant interest in the synthesis of one-dimensional semiconductor nanomaterials such as GaN nanowires, MgO nanowires, SnO_2 nanowires, and ZnO nanowires due to various remarkable physical and chemical properties distinctive from conventional bulk materials [1–7]. Because zinc oxide is a wide band gap (3.37 eV) semiconductor with a large exciton binding energy of 60 meV, its nanomaterials have attracted extraordinary attention for their potential applications in device and interconnect integration in nanoelectronics and molecular electronics [8–12]. Various kinds of

*Corresponding author. Tel.: +86 1082648035; fax: +86 1062556598.
E-mail addresses: lf@aphy.iphy.ac.cn (F. Liu), hjgao@aphy.iphy.ac.cn (H.J. Gao).

0022-0248/$ - see front matter © 2004 Elsevier B.V. All rights reserved.
doi:10.1016/j.jcrysgro.2004.09.080

techniques have been developed to synthesize the single crystalline ZnO nanowires [13–19]. For example, Huang et al. [13] prepared the aligned ZnO nanowire arrays on a sapphire covering Au film by a carbon thermal-reduction chemical vapor transport and condensation method at 800–1000 °C, Kong et al. [14] fabricated ZnO nanowire arrays by evaporation of a mixture of Zn and Se powders at 1100 °C, and Wang et al. [15] synthesized ZnO nanowires by oxidation of Zn powders mixed with Au nanoparticles at 900 °C. Using nickel nitrate as catalyst, Lyu et al. [18] also grew ZnO nanowires at 500 °C. Up to now, few studies have been reported on the subject of catalyst-free fabrication of ZnO nanowire and nanorod arrays at temperature below 600 °C [16,20]. Furthermore, the presence of catalyst is also harmful to its applications in nanodevice and high-temperature growth technique will limit the fabrication of ZnO nanomaterials in gentle circumstance. Therefore, growth method at low-temperature and without catalyst becomes an important research subject in nanotechnology.

In this Letter, at low temperature of about 550 °C and without catalyst, large areas, well-aligned ZnO nanorods and nanowires, have been synthesized on porous silicon in a simple single-stage furnace. The morphologies, structures and optical properties of ZnO nanowires and nanorods were characterized by scanning electron microscopy (SEM), transmission electron microscopy (TEM), X-ray diffraction (XRD), and photoluminescence (PL) measurements.

2. Experimental procedure

Porous silicon substrates were obtained by electrochemical etching of Si (1 1 1) wafers (P type, 0.004–0.007 Ω cm) in electrolyte which is a mixture of hydrofluoric acid, distilled water and ethanol. The current density was kept at 10 mA/cm^2 for 10–30 min. A thin nanoporous layer would be formed on the surface of a silicon wafer. Large scale, aligned ZnO nanorods and nanowires in these experiments were grown by a simple vapor evaporation method developed in our group [21]. The only difference in our method is that, sites A and B refer to the upstream of the gases flow and the center of the furnace, respectively. Zinc powders (99.99%), as the source materials, were placed in a quartz vessel that was inserted in a single-stage furnace. The temperature, gas flow rate and evaporation rate of B region could be controlled. Oxygen gas was not fed into the reaction region until the temperature of the furnace was ramped to 550 °C. For ZnO nanorod and nanowire, the oxygen flow rate was kept at 10 and 20 sccm through all the processes, respectively. At the same time, the flow rate of argon gas was controlled at a constant rate (200 sccm). After evaporation for 30 min in an atmosphere of argon and oxygen gas, white fluffy materials were formed on porous silicon surface.

A field-emission type scanning electron microscope (XL-SFEG, FEI Corp.) was used to observe the morphologies of the ZnO nanostructures. TEM (Tecnai-20, PHILIPS) and high-resolution transmission electron microscope (Tecnai F20, FEI Corp.) were used to provide TEM images of ZnO nanostructures, respectively. XRD data was obtained on a Rigaku D/MAX 2400 type spectroscopy and Cu $K_{\alpha 1}$ radiation was used (wavelength 1.5406 Å). PL measurement was performed at room temperature on a HITACHI F-4500 type spectrophotometer with He–Cd laser as the excitation light with wavelength of 325 nm.

3. Results and discussion

In our previous work, controlled self-assembled growth of ZnO nanoplanes, tetrapodlike ZnO networks, and ZnO nanocombs have been synthesized by simple oxidation of Zn powders [22]. By varying experimental condition, large areas of aligned ZnO nanowires could be obtained. SEM and TEM images of the ZnO nanowires fabricated on porous silicon at 550 °C are shown in Fig. 1. Fig. 1A shows that ZnO nanowires of high density are synthesized in the orientation perpendicular to the substrate surface. In Fig. 1B, it can be seen that these nanowires have uniform diameter of about 40 nm and length up to 2 μm, resulting in the average aspect ratio estimated about 50. Typical TEM image of the ZnO nanowires is shown in

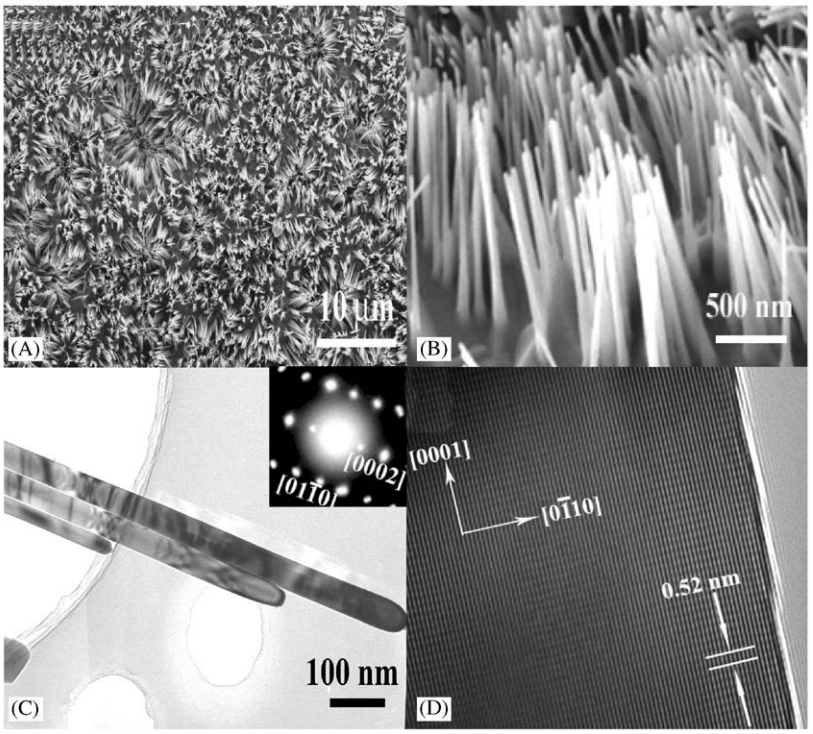

Fig. 1. SEM and TEM images of ZnO nanowires. (A, B) Low and high magnification SEM images of ZnO nanowires. (C) TEM image of a typical ZnO nanowire. The inset is the SAED pattern from an individual ZnO nanowire. (D) HRTEM image of an individual ZnO nanowire showing lattice image of the perfect single crystalline structure and its crystalline orientation.

Fig. 1C. It is found that the ZnO nanowires display elliptic head shapes and grow along [0 0 0 1] axis as shown in the inset of Fig. 1C, not [1 1 $\bar{2}$ 0] [23]. Fig. 1D is a high-resolution transmission electron microscopy (HRTEM) image taken from an individual ZnO nanowire, which shows the perfect single crystalline structure and confirms that the ZnO nanowire is a wurtzite structure with lattice constants of $a = 0.324$ nm and $c = 0.519$ nm.

By continuing to vary the ratio of flow rates of argon to oxygen gas, high-density aligned ZnO nanorods have also been successfully grown at 550 °C. Fig. 2 are SEM and TEM images of the aligned ZnO nanorods synthesized. It is observed that almost all the ZnO nanorods are vertical to the porous silicon surface in Fig. 2A. From Fig. 2B we can see that the ZnO nanorods are about 90 nm in diameter and 2 μm in length, and the average aspect ratio is estimated to be about 20. The inset in Fig. 2B provides a typical morphology of nanorods with hexagonal symmetry. We can find that all the ends of the ZnO nanorods are well faceted, which can serve as mirror planes for the laser cavities as described in Ref. [13]. It is the main morphology difference between the ZnO nanorods and nanowires that nanorod has a regular hexagonal shape, while nanowire does not. From Fig. 2C it can be observed that the ZnO nanorods have single-crystalline structure and grow along [0 0 0 1] axis as shown in the inset (Fig. 2C). HRTEM image (Fig. 2D) displays that ZnO nanorod has a perfect wurtize structure just like the ZnO nanowire.

The possible growth mechanism of the ZnO nanowire and nanorod arrays is vapor–solid (VS) mechanism because no metal catalyst was used in the whole evaporation procedure. But the mechanism of aligned growth of ZnO is still an open question and needs further study. Many proposed mechanisms have been developed, such as

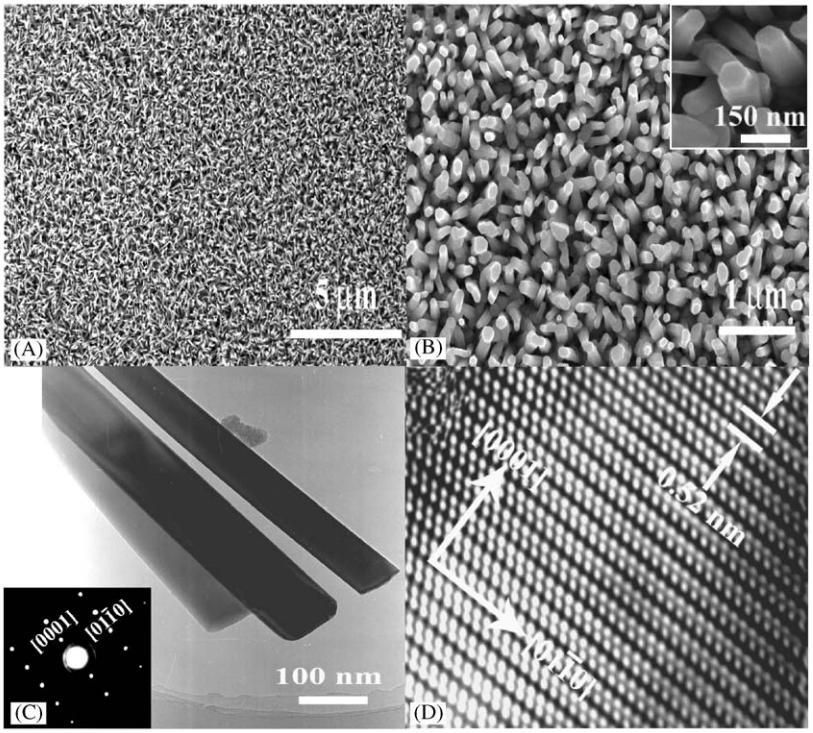

Fig. 2. SEM and TEM images from ZnO nanorods. (A, B) Low and high magnification SEM images of ZnO nanorods. The inset (in Fig. 2B) shows typical top-end morphology of the ZnO nanorods. (C) TEM image from an individual ZnO nanorod. The SAED pattern of an individual ZnO nanorod is shown in the inset. (D) HRTEM image of an individual ZnO nanorod indicating the perfect wurtize structure.

constraint of the pores in either mesoporous silicon [25] or porous anodic alumina [26], Van der Waals interaction [27], effects of DC bias [28]. In this paper, we have synthesized well-aligned ZnO nanorod and nanowire arrays on porous silicon without using any catalysts. The alignment mechanism is not the constraint of the pores because the core diameter of porous silicon prepared is about 1–2 μm, which is much wider than the distance between the nanorods or nanowires (50–150 nm). Moreover, the distance of the arrays is also beyond the range of Van der Waals interaction, so the possible aligned mechanism in our work may be attributed to steric overcrowding [21].

To further understand the influence of the morphology difference on the properties of nanostructures, XRD is used to study the crystalline

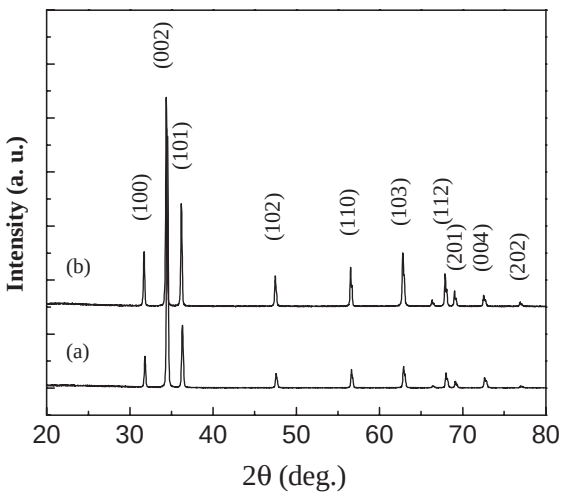

Fig. 3. XRD pattern of ZnO nanowires and nanorods on porous silicon: (a) ZnO nanorods and (b) ZnO nanowires.

structure and the crystalline alignment. Fig. 3 gives the XRD patterns of the ZnO nanowires (a) and the ZnO nanorods (b). It is known that the easy growth axis of one-dimensional ZnO nanomaterials is [0 0 0 1] and as the alignment of ZnO arrays improves, the diffraction peaks other than (0 0 0 1) begin to disappear accordingly [13]. From Fig. 3 we can see that the diffraction peaks other than (0 0 0 1) of ZnO nanowires show higher relative intensity than those of the ZnO nanorods. It indicates that the alignment of the nanorods is better than that of nanowires. According to the standard XRD pattern, both the ZnO nanowires and the ZnO nanorods are wurtzite structure, which is in agreement with the TEM results (Figs. 2C and D, 3C and D).

Optical properties of these nanostructures are investigated. As shown in Fig. 4, ZnO nanorods and nanowires correspond to different PL properties. A high-intensity narrow UV peak at 381.2 nm wavelength and a low-intensity broad green peak at 492.8 nm wavelength are observed from the curve (Fig. 4(b)) of ZnO nanowires at room temperature. For the ZnO nanorods, the UV peak appearing at 383.8 nm wavelength in Fig. 4(a) shows a slight shift to low frequency in comparison with the ZnO nanowires. The UV emission corresponds to the near band-edge emission, namely the recombination of free excitons through an exciton–exciton collision process [14]. The slight shift in UV emission is possible because the tensile strain turns more intensive as the diameter of the ZnO nanostructure increases [23]. The green transition referred to a deep-level or trapped-state emission is attributed to the green transition of the single ionized oxygen vacancy in ZnO. It implies that the radiative recombination of a photon generates hole with an electron occupying the oxygen vacancy [30]. From the PL spectra of these nanomaterials, it is found that the intensity of the green emission decreases while the UV emission increases from nanowire to nanorod. Since higher intensity of the green luminescence corresponds to more oxygen vacancies, the progressive decrease of the green emission relative to the UV emission suggests the ZnO nanorods have higher crystallization and less oxygen vacancy concentrations than the ZnO nanowires. Obviously, by controlling the morphology of ZnO nanostructures, the optical property of the ZnO nanostructures can be tunable, which will be useful for nanolaser applications.

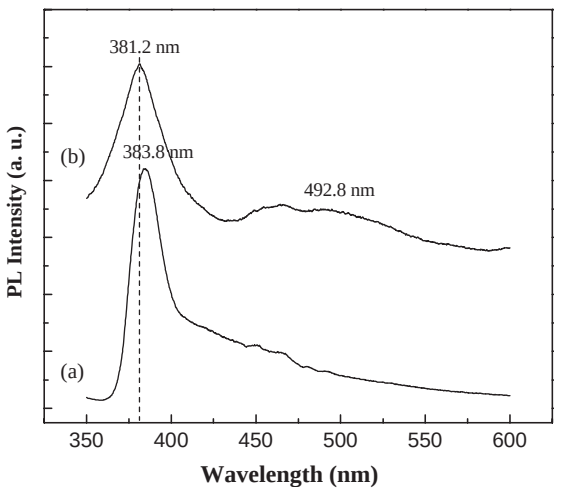

Fig. 4. Photoluminescence spectra of ZnO nanowires and nanorods at room temperature: (a) ZnO nanorods and (b) ZnO nanowires.

4. Conclusion

In conclusion, we have synthesized large-scale aligned ZnO nanorods and nanowires without using catalyst and at a relative low temperature of ~550 °C by simple oxidation of Zn powders. All of these nanorods and nanowires display perfect single crystalline structure. With the improvement of ZnO crystallization, a lower concentration of oxygen vacancies is present in these ZnO nanomaterials. This no-catalyst growth technique at low-temperature may have a potential application for fabricating nanoelectronic and nanooptical devices.

Acknowledgements

The authors would like to thank Prof. Zhonglin Wang for helpful discussion. This work was supported by the National 863 and 973 projects, and the National Science Foundation of China

with Grant Nos. 90201036, 60125103, 60228005, and 90206028.

References

[1] W.Q. Han, S.S. Fan, Q.Q. Li, Y.D. Hu, Science 277 (1997) 1287.
[2] S.S. Wong, E. Joselevich, A.T. Woolley, C.L. Cheun, C.M. Lieber, Nature 394 (1998) 52.
[3] Y. Cui, Q.Q. Wei, H.K. Park, C.M. Lieber, Science 293 (2001) 1289.
[4] J. Wang, M.S. Gudiksen, X. Duan, Y. Cui, C.M. Lieber, Science 293 (2001) 1455.
[5] P. Yang, C.M. Lieber, Science 273 (1996) 1836.
[6] Y.L. Wang, X.C. Jiang, Y.N. Xia, J. Am. Chem. Soc. 125 (2003) 16176.
[7] Y.N. Xia, P.D. Yang, Y.G. Sun, Y.Y. Wu, B. Mayers, B. Gates, Y.D. Yin, F. Kim, H.Q. Yan, Adv. Mater. 15 (2003) 353.
[8] R.H. Baughman, A.A. Zakhidov, W.A. Hee, Science 297 (2002) 787.
[9] J. Hu, T.W. Odom, C.M. Lieber, Acc. Chem. Res. 32 (1999) 435.
[10] Z.W. Pan, Z.R. Dai, Z.L. Wang, Science 291 (2001) 1947.
[11] J.R. Heath, P.J. Kuekes, G. Synder, R.S. Williams, Science 280 (1998) 1717.
[12] D. Snoke, Science 273 (1996) 1351.
[13] M.H. Huang, Y. Wu, H. Feick, N. Tran, E. Weber, P. Yang, Adv. Mater. 13 (2001) 113.
[14] Y.C. Kong, D.P. Yu, B. Zhang, W. Fang, S.Q. Feng, Appl. Phys. Lett. 78 (2001) 407.
[15] Y.W. Wang, L.D. Zhang, G.Z. Wang, X.S. Peng, Z.Q. Chu, C.H. Liang, J. Crystal Growth 234 (2002) 171.
[16] W.I. Park, D.H. Kim, S.W. Jung, Gyu-Chui. Yi, Appl. Phys. Lett. 80 (2002) 4232.
[17] Z.L. Wang, R.P. Gao, Z.W. Pan, Z.R. Dai, Adv. Eng. Mater. 3 (2001) 657.
[18] S.C. Lyu, Y. Zhang, H. Ruh, H.J. Lee, H.W. Shim, E.K. Suh, C.J. Lee, Chem. Phys. Lett. 363 (2002) 134.
[19] M.J. Zheng, L.D. Zhang, G.H. Li, W.Z. Shen, Chem. Phys. Lett. 363 (2002) 123.
[20] W.I. Park, Gyu-Chui. Yi, M.Y. Kim, S.J. Pennycook, Adv. Mater. 15 (2003) 526.
[21] P.J. Cao, Y.S. Gu, H.W. Liu, F. Shen, Y.G. Wang, Q.F. Zhang, J.L. Wu, H.J. Gao, J. Mater. Res. 18 (7) (2003) 1686.
[22] F. Liu, P.J. Cao, H.R. Zhang, J.Q. Li, H.J. Gao, Nanotechnology 15 (2004) 949.
[23] J.S. Lee, K. Park, M.I. Kang, I.W. Park, S.W. Kim, W.K. Cho, H.S. Han, S.S. Kim, J. Crystal Growth 254 (2003) 423.
[25] W.Z. Li, H. Zhang, C.Y. Wang, Y. Zhang, L.W. Xu, K. Zhu, Appl. Phys. Lett. 70 (1997) 2685.
[26] S.H. Tsai, F.K. Chiang, T.G. Tsai, F.S. Shieu, H.C. Shih, Thin Solid Films 366 (2000) 11.
[27] S.S. Fan, M.G. Chapline, N.R. Franklin, T.W. Tombler, A.M. Cassell, H.J. Dai, Science 283 (1999) 512.
[28] Y. Chen, D.T. Shaw, L.P. Guo, Appl. Phys. Lett. 76 (2000) 2469.
[30] K. Vanheusden, W.L. Warren, C.H. Seager, D.R. Tallant, J.A. Voigt, B.E. Gnade, J. Appl. Phys. 79 (1996) 7983.